

Segmental Orientation in Well-Defined Thermoplastic Elastomers Containing Supramolecular Fillers

Eva Wisse,[†] A. J. H. Spiering,[†] Frank Pfeifer,[‡] Giuseppe Portale,[§] H. W. Siesler,[‡] and E. W. Meijer^{*,†}

Laboratory of Macromolecular and Organic Chemistry, Eindhoven University of Technology, P.O. Box 513, 5600 MB Eindhoven, The Netherlands, Department of Physical Chemistry, University of Duisburg-Essen, D 45117 Essen, Germany, and Netherlands Organisation for Scientific Research (NWO), DUBBLE@ESRF, Grenoble F-38043, France

Received July 23, 2008; Revised Manuscript Received November 21, 2008

ABSTRACT: The mechanical behavior of segmented block copolymers is studied by unraveling the deformation mechanisms on both a macroscopic and a molecular level. Small-angle X-ray scattering and infrared dichroism are used to study the deformation of a thermoplastic elastomer with bisureidobutylene hard segments (PCLU4U) containing various amounts of perfectly fitting supramolecular filler (U4U) incorporated. The pristine PCLU4U and polymers containing filler amounts up to 25 mol % show predominantly a shear type of deformation. The hard segment stacks tend to align parallel to the strain axis upon uniaxial deformation up to the yield point. Permanent deformation is caused by fragmenting of the stacks, which then start to reorient perpendicular to the strain axis. When >25 mol % of filler is added to PCLU4U, two hard phases are present: the first hard phase consists of polymer hard segments containing a maximum amount of filler incorporated and the second hard phase consists of filler aggregates only. In this case, all urea groups orient parallel to the strain axis when such a sample is uniaxially loaded up to the yield point. At the yield point, the first hard phase shows the same shear type of deformation as the pure PCLU4U polymer. The filler aggregates, however, are not connected to the soft segment matrix, and stress transfer to the soft matrix does not occur. Therefore, we propose that they remain parallel to the strain axis. All of these data support the unique character of the supramolecular fillers used in well-defined thermoplastic elastomers.

Introduction

The domain morphology of microphase separation between hard and soft domains in thermoplastic elastomers (TPEs) has been extensively studied to explain their mechanical behavior. The first report on morphological changes during deformation of segmented polyurethanes (PUs) was by Bonart.^{1,2} He studied PUs with small-angle X-ray scattering (SAXS) and proposed a molecular interpretation for his systems. In later studies, SAXS was often used.^{3,4} However, to gain more insight into the molecular level, infrared (IR) polarization spectroscopy proved to be very useful.^{5–12} Gaymans¹³ specifically studied the deformation behavior of segmented block copolymers with well-defined hard segments. Ideally, SAXS and transmission IR dichroism experiments are combined to study the deformation at the macroscopic domain level and the molecular level, respectively.^{14–16}

For the uniaxial deformation of PUs or polyurethaneureas, various deformation mechanisms, typically for lamella-type hard domains, are described. Two extremes of deformation mechanisms are reported.¹⁴ In the first mechanism, the long axis of the hard domain orients parallel to the applied force at low strains, combined with orientation of the soft segment chains in the same direction. When the stress is transferred from the hard to the soft segments, permanent deformation starts to occur, causing hard segment fragmentation. The hard domains now orient perpendicular to the applied force. This principle is described by Desper et al. as the shear model.⁴ In a second mechanism, the hard domains are oriented with their long axis perpendicular to the tensile direction and the soft segment chains are pulled apart at low strains (affine deformation). When the

soft segments are sufficiently extended, the stress is transferred from the soft segments to the hard domains, causing the hard domains to fragment. This mechanism is described as the tensile mode by Desper et al.⁴ In this case, the hard domains are always oriented perpendicular to the applied force. Desper et al. conclude that the shearing mechanism is predominant in their amine-cured PU, where the hard domains have a good structural integrity. A high degree of crystallinity of the hard segments is also reported to cause the orientation behavior by Lin et al. following the shearing mechanism.⁶ The diol-cured PU from Desper et al. possesses weaker hydrogen bonds in the hard domains and predominantly shows deformation behavior according to the tensile mode. Lee et al.^{14,15} describe the deformation of their PU as a combination of both processes. This seems to be the case in many reports because a mostly negative value for the orientation function is observed at lower strains, which again increases in value when permanent deformation sets in.^{6–8,10,15} (See the Experimental Section for a description of the orientation function, *f*.)

We recently reported the concept of supramolecular reinforcement fillers that are incorporated into PCLU4U (Figure 1) TPEs containing monodisperse bisureidobutylene hard segments.¹⁷ In the regime up to ~24 mol % of filler, polymer and filler were shown to form a single hard phase because of the perfect fit between the hydrogen-bonding sequence of the filler and the polymer. When >24 mol % of filler was mixed in the polymer, a second regime was entered in which a separate filler hard phase was observed besides the filler-saturated polymer hard phase. The transition from the first to the second regime occurs via a less-defined transition regime. Incorporation of 24 mol % resulted in an *E* modulus increase from 12 to 29 MPa without a decrease in tensile strength or strain at break. When >24 mol % was incorporated, the tensile strength and strain at break strongly decreased, which was attributed to oversaturation of the polymer hard phase with filler and the presence of an

* Corresponding author: E-mail: E.W.Meijer@tue.nl.

[†] Eindhoven University of Technology.

[‡] University of Duisburg-Essen.

[§] DUBBLE@ESRF.

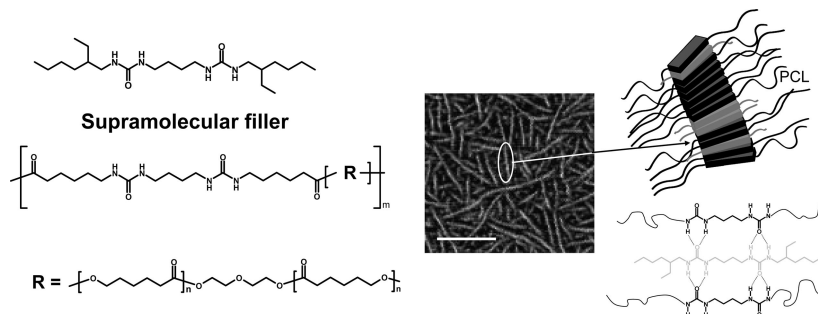


Figure 1. Modular approach. The supramolecular filler (gray) is incorporated into the PCLU4U hard domains (black) via bifurcated hydrogen bonds. The AFM phase image shows the nanoribbon morphology of the hard segment stacks (scale bar is 100 nm).

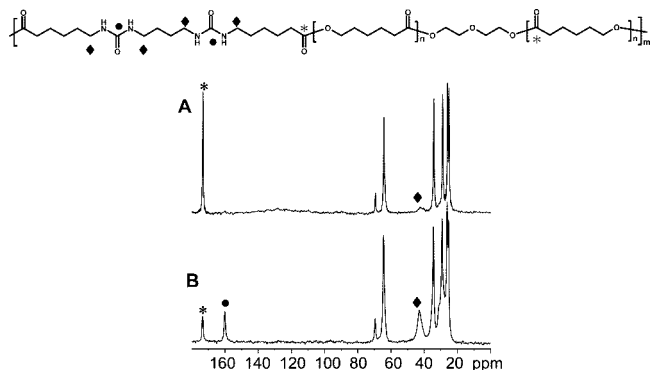


Figure 2. Solid-state ^{13}C NMR spectra selecting either (A) mobile phase (direct ^{13}C excitation) or (B) rigid phase of PCLU4U (^1H – ^{13}C cross-polarization).

additional separate filler phase. In this Article, the orientation behavior of PCLU4U upon uniaxial deformation with increasing amounts of supramolecular filler incorporated via a modular approach (Figure 1) is studied by a combination of dichroic IR and SAXS measurements. In this way, the remarkable mechanical properties reported before can be explained.

Results and Discussion

Phase Separation between Hard and Soft Segments in PCLU4U. Before studying the orientation behavior of the hard segment nanoribbons, we investigated the extent of phase separation between hard and soft segments. IR data presented earlier¹⁸ showed evidence of only strongly hydrogen-bonded urea units in PCLU4U up to the melting point of the hard segments (urea: $\text{C}=\text{O} \approx 1620 \text{ cm}^{-1}$ and $\text{N}-\text{H} \approx 3330 \text{ cm}^{-1}$). This implies that there are no bisurea segments dissolved in the soft matrix, and phase separation between hard and soft segments is complete. A relatively new method for studying phase separation is solid-state NMR spectroscopy.¹⁹ Direct-excitation ^{13}C NMR experiments applying the appropriate interscan delay select the more mobile carbons (Figure 2A), whereas ^1H – ^{13}C cross-polarization experiments select the rigid carbons (Figure 2B). Accurate resolution was reached for both carbonyl carbons (* and ● in Figure 2) and for the CH_2 groups next to the urea (◆). The carbonyl carbon of the PCL soft segment is observed in the direct-excitation ^{13}C spectrum. In the ^1H – ^{13}C cross-polarization experiments, this peak is strongly reduced,²⁰ whereas the carbonyl carbon of the urea has appeared. Also, the signal of the CH_2 groups next to the urea has strongly increased. The fact that no urea carbonyl signals are observed in the mobile phase especially confirms that, within the experimental error of the measurement, no bisurea segments are dissolved in the soft matrix. All bisurea units are therefore involved in hard-segment nanoribbon formation.

Infrared Dichroic Measurements. Thin films (typically $\sim 20 \mu\text{m}$ thick) of PCLU4U with varying amounts of supramolecular filler were prepared by casting from chloroform solutions. The samples were stretched at 10 mm/min while the IR spectra were recorded using polarized radiation alternately changed between the parallel and perpendicular directions with respect to the deformation axis. All measurements were performed at 37 °C to ensure a completely molten PCL soft segment. From the recorded IR spectra, we calculated the dichroic ratio R

$$R = \frac{A_{\parallel}}{A_{\perp}} \quad (1)$$

The state of orientation can be expressed by the orientation function, f

$$f = \frac{3\langle \cos^2 \beta \rangle - 1}{2} \quad (2)$$

In this equation, β is the angle between the main chain axis and the deformation axis. The orientation function is related to the dichroic ratio by

$$f = \frac{(R-1)(R_0+2)}{(R_0-1)(R+2)} \quad (3)$$

$$R_0 = 2 \cot^2 \psi \quad (4)$$

R_0 is the dichroic ratio for perfect uniaxial orientation, and ψ is the angle between the transition moment of the vibrating oscillator and the polymer chain axis. The upper and lower limits of eq 3 are defined by eq 2 and result in $f = 1$ for parallel alignment of the chains and $f = -1/2$ for perpendicular alignment. In the case of random orientation, $f = 0$.

The IR spectra of PCLU4U have already been discussed in detail.¹⁸ In the dichroic IR measurements, we predominantly used the $\text{N}-\text{H}$ bands of the urea to calculate R and f . Also, the $\text{C}=\text{O}$ band of the urea was used; however, because of the large difference between the intrinsic intensities of these two signals, the $\text{C}=\text{O}$ intensity was often too high for the detector used. Therefore, only the results of the $\text{N}-\text{H}$ groups are reported. In all cases in which we could calculate the orientation function on the basis of the $\text{C}=\text{O}$ of the urea, the same orientation behavior was observed (data not shown). Figure 3 shows typical examples of a recorded engineering stress–strain curve of PCLU4U and of orientation functions of four samples with various filler contents (0, 10, 24, and 51 mol %) as a function of strain during a dichroic IR measurement. Because of the dimensions of the setup, a maximum elongation of $\sim 550\%$ could be reached. All samples started with a random orientation ($f = 0$), as expected from previous AFM studies.¹⁷

In PCLU4U without any additional filler, the orientation function became negative when elongation started, indicating that the urea $\text{N}-\text{H}$ groups and therefore also the nanoribbons were oriented parallel to the strain axis. This orientation became

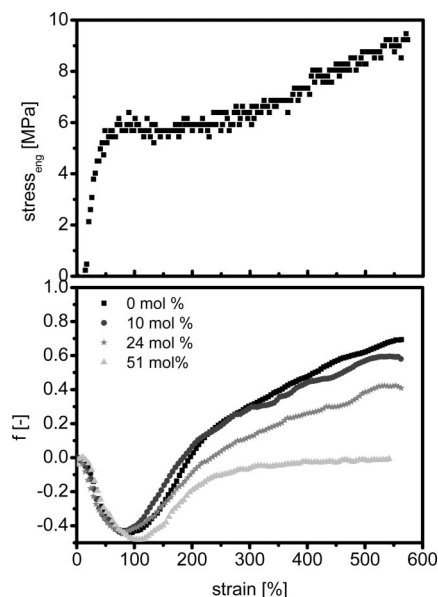


Figure 3. Representative stress–strain curve (PCLU4U, no filler) and corresponding orientation functions of N–H vibration of PCLU4U containing various amounts of supramolecular filler.

stronger upon approaching the yield point and almost reached its theoretical minimum value of -0.5 at the yield point, indicating excellent orientation of the bisurea nanoribbons. In duplo experiments, the minimum value of -0.5 for f was sometimes a little higher, which we attribute to small differences in sample preparation. According to Fischer and colleagues, this type of deformation mechanism indicates that rotation of the hard segments occurs without substantial interdomain interactions.¹¹ Considering the low hard-block content of 10.6 wt %, the Fischer model provides an attractive interpretation of the behavior of PCLU4U. When the yield point was reached at $\sim 100\%$ strain, permanent deformation set in, and concurrently, the orientation function started to increase again. Values up to 0.7 at 550% elongation were reached. When we keep in mind that PCLU4U can be elongated over 3000% under these conditions,¹⁷ already a high degree of order is reached at this moderate elongation. These observations correspond to a shear mode deformation mechanism for PCLU4U. In this model, the perpendicular orientation of the hard segment stacks after the yield point is explained by fragmenting of the stacks, after which the stress is transferred from the hard segments to the soft segments. The smaller stacks therefore twist toward an orientation perpendicular to the strain axis. This theory is confirmed when looking at various IR spectra during the tensile tests. In the IR spectra of PCLU4U at 15, 275, and 560% strain (Figure 4), we see a free N–H band at 3405 cm^{-1} appearing at 275% strain. This corresponds nicely with more free N–H groups at the ends of the ribbons due to fragmenting of the nanoribbons. This band is more intense at greater elongation (560% strain), indicating increased fragmentation into smaller hard segment stacks. An additional explanation could be that some hard segments are pulled into the soft matrix.¹⁰

The orientation function as a function of strain for PCLU4U with 10 mol % of supramolecular filler is similar to that of PCLU4U. Filler and polymer hard block remain a single hard phase during uniaxial loading, as was already suggested to explain the remarkable mechanical behavior in this first regime. In the second regime, the deformation behavior is different. When 51 mol % of filler was mixed into the polymer, all urea groups oriented in the direction of the applied force up to the yield point. Upon elongating beyond the yield strain, the orientation function also increased in value. However, the

maximum value reached was now ~ 0 . A sudden random orientation of the urea is not likely. We propose that beyond the yield point the polymer hard phase (including a maximum amount of incorporated filler) fragments and orients perpendicular to the applied strain, similar to what was just described. However, because the filler phase is not connected to the PCL matrix, we propose that the filler stacks remain in their previous orientation. In total, we have nanoribbons of one hard phase (polymer hard segments including a maximum amount of filler) oriented perpendicular to the applied force, whereas the second hard phase (filler stacks) remains oriented parallel to the tensile direction. The sum of the orientation functions of these two phases will lead to an orientation function, as observed in Figure 2 for PCLU4U containing 51 mol % of filler. When 24 mol % was mixed into PCLU4U, we observed intermediate behavior. The curve still mostly resembles the behavior of the pure polymer, but its final value for f has already somewhat decreased. This is once more an indication of a less-defined transition regime when going from the first to the second regime.¹⁷

The orientation of the soft segment was studied by integrating the C=O bands of the PCL at 1720 cm^{-1} . Remarkably, we never observed any orientation opposed to what is generally stated in literature.^{5,6,8–10,14,15} For polymers with the same hard segment but a poly(tetrahydrofuran) soft segment, the soft segment also did not orient upon uniaxial elongation.²¹ Moreland et al. also observed no orientation of poly(propylene oxide) soft segments in his polyurethaneurea.⁷ They attributed this to the entropy-driven relaxation of the soft segments leading to more disorder.

Beyond the yield point, plastic deformation starts because of fragmentation of the hard segment nanoribbons. This was shown by elongating a sample of PCLU4U to 530% strain under the same conditions as those just described. At certain elongations, the experiment was stopped and the sample was held at this position while we kept recording IR spectra alternately parallel and perpendicular to the strain axis (Figure 5A). The orientation function remained at the final value of 0.7. When we stopped the experiment at 50% strain, the hard segment stacks showed some relaxation. The orientation function increased in value, though not all of the way back to the initial situation of $f = 0$ in the time span used for the measurement (Figure 5B).

Small-Angle X-ray Scattering. Deformation at the macroscopic level was studied by SAXS. Samples of 0.5 to 1.0 mm thickness were elongated at 10 mm/min in a tensile setup at 37°C up to a certain elongation, after which SAXS images were acquired using a 2D detector. The SAXS patterns show a d spacing (average internanoribbon distance) of $\sim 6\text{ nm}$ for all samples before elongation (Figure 6). The SAXS intensity is clearly lower for 23 and 50 mol % samples than for 0 and 10 mol % samples. This is most probably due to a decrease in the electron density difference between the hard segment stacks and the matrix with increasing filler content. The corresponding circular scattering halos are presented in Figure 7, confirming random orientation of the hard segment stacks at 0% strain. All samples were stretched up to strains below (50%), at (100%), and over the yield point (300 or 400%) and were then kept at that elongation after which SAXS images were recorded for 5 min to obtain patterns with a good resolution (Figure 7). The pure polymer and the sample containing 10 mol % of filler again showed very similar behavior upon elongation. At 50% strain, an ellipsoid pattern was observed, indicating that the distance between hard segment stacks (long period) was increased in the strain direction and that the hard segment stacks were more orientated in the strain direction. At 100% strain, we observed a four-point scattering pattern. Such pattern indicates that the hard segment stacks are oriented more parallel to the strain axis. Also, a superimposed scattering halo was still observed,

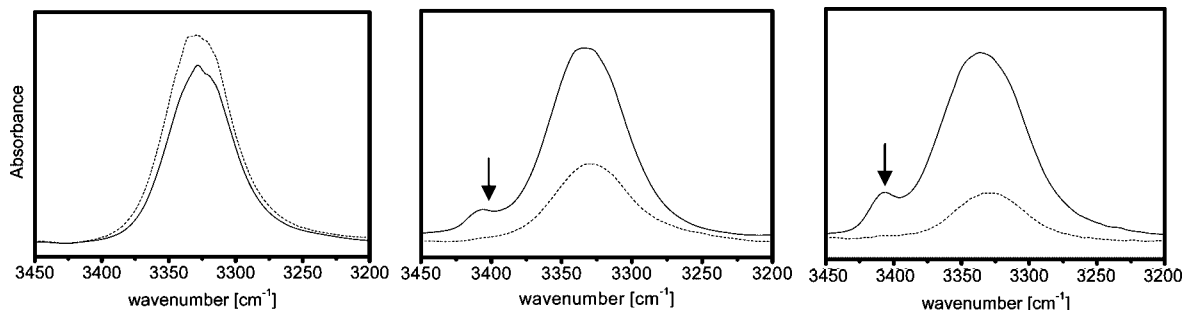


Figure 4. Zoom of IR spectra in N–H stretching region of PCLU4U at (A) 15, (B) 275, and (C) 560% strain. Dashed curve: recorded parallel to tensile direction; solid curve: recorded perpendicular to tensile direction. The arrow indicates the free N–H band.

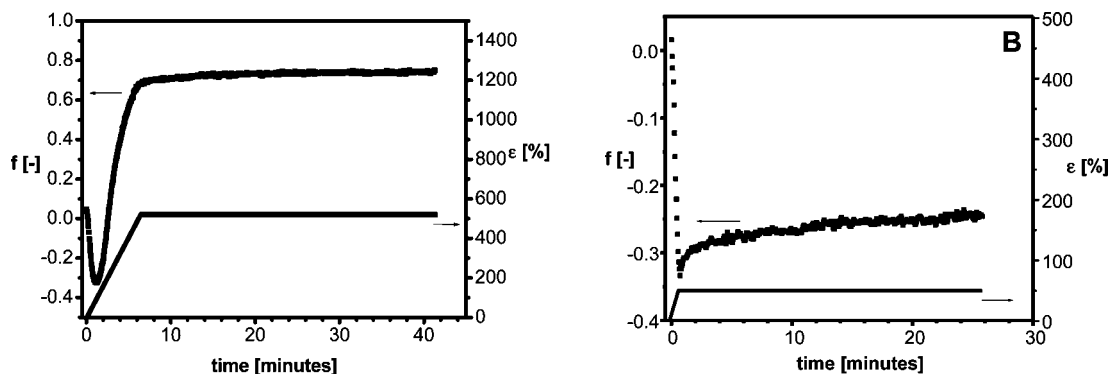


Figure 5. Orientation function of N–H vibration over time. End of tensile test at (A) 520 and (B) 50% strain.

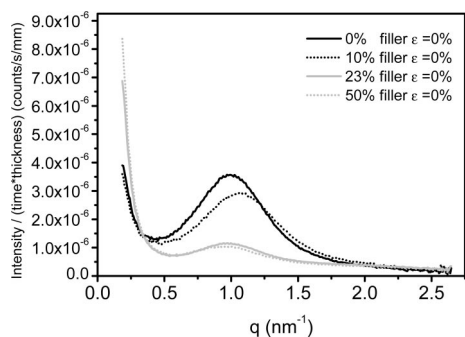


Figure 6. SAXS patterns of PCLU4U with various amounts of incorporated filler; d spacings ($= 2\pi/q$) are 6.3, 5.9, 6.5, and 6.7 nm, respectively.

indicating the presence of still more randomly distributed stacks. At 400% strain, a two-point pattern along the direction parallel to the strain axis was observed, showing that the nanoribbons were now oriented perpendicular to the strain axis. The SAXS data confirmed the orientation behavior as deduced from the dichroic IR measurements for samples containing 0 and 10 mol % of supramolecular filler (first regime).

For the samples containing 23 and 50 mol %, transition and second regime respectively, we basically observe the same behavior. Additionally, a clear horizontal streak is observed at strains over the yield point in both samples. This is most clearly observed in PCLU4U containing 50 mol % filler. These horizontal streaks are most probably caused by filler aggregates that are aligned parallel to the strain axis. We also recorded SAXS patterns during tensile tests at 1 mm/min. These dynamic studies resulted in images with a lower resolution (data not shown). However, the results did show similar scattering patterns, as shown in Figure 7, showing only horizontal streaks in the highest stretched samples containing 23 and 50 mol % filler. This indicates that the static

measurements are a good representation of the dynamic processes.

The results from the IR and SAXS measurements presented in the previous sections both support the same model of U4U nanoribbon orientation during uniaxial elongation. Figure 8 schematically summarizes the nanoribbon deformation, showing the polymer U4U hard segments in black and the filler U4U segments in gray.

Conclusions

In PCLU4U, the bisurea hard segments (10.6 wt % HB) are completely phase separated from the soft PCL matrix. The ribbon-to-ribbon distance in unloaded samples is on average ~ 6 nm. In AFM, we observe ribbons with a monodisperse diameter, pointing to hard segment stacks with similar width and thickness. We propose that supramolecular bisurea ribbons (Figure 9A) stack on top of each other because of dipole–dipole interactions between the urea groups. Most probably, a single hard segment stack, as visualized in AFM images, consists of a few supramolecular ribbons crystallized together (Figure 9B) in a nanoribbon with similar width and thickness.

When PCLU4U is uniaxially strained, a shear-type deformation mechanism is observed for the hard segment nanoribbons in both dichroic IR and SAXS experiments. We attribute this to the strong hydrogen bonds between bisurea units, as already suggested in literature,^{4,6} combined with very little interdomain interaction between hard domains.¹⁵ The soft segment does not show any preferred orientation during stretching up to 550% strain, possibly because of relatively fast relaxation of the soft segment chains.⁷ When 10 mol % of supramolecular filler was added to the poly(urea), the exact same mechanism was observed. This confirms that during uniaxial loading of this material, the filler and polymer hard segments remain a single hard phase. PCLU4U containing 50 mol % of filler displays different behavior. Up to the yield point, all urea groups orient parallel to the strain axis. When fragmentation of the nanoribbons sets in, stress is transferred from the hard segments to the

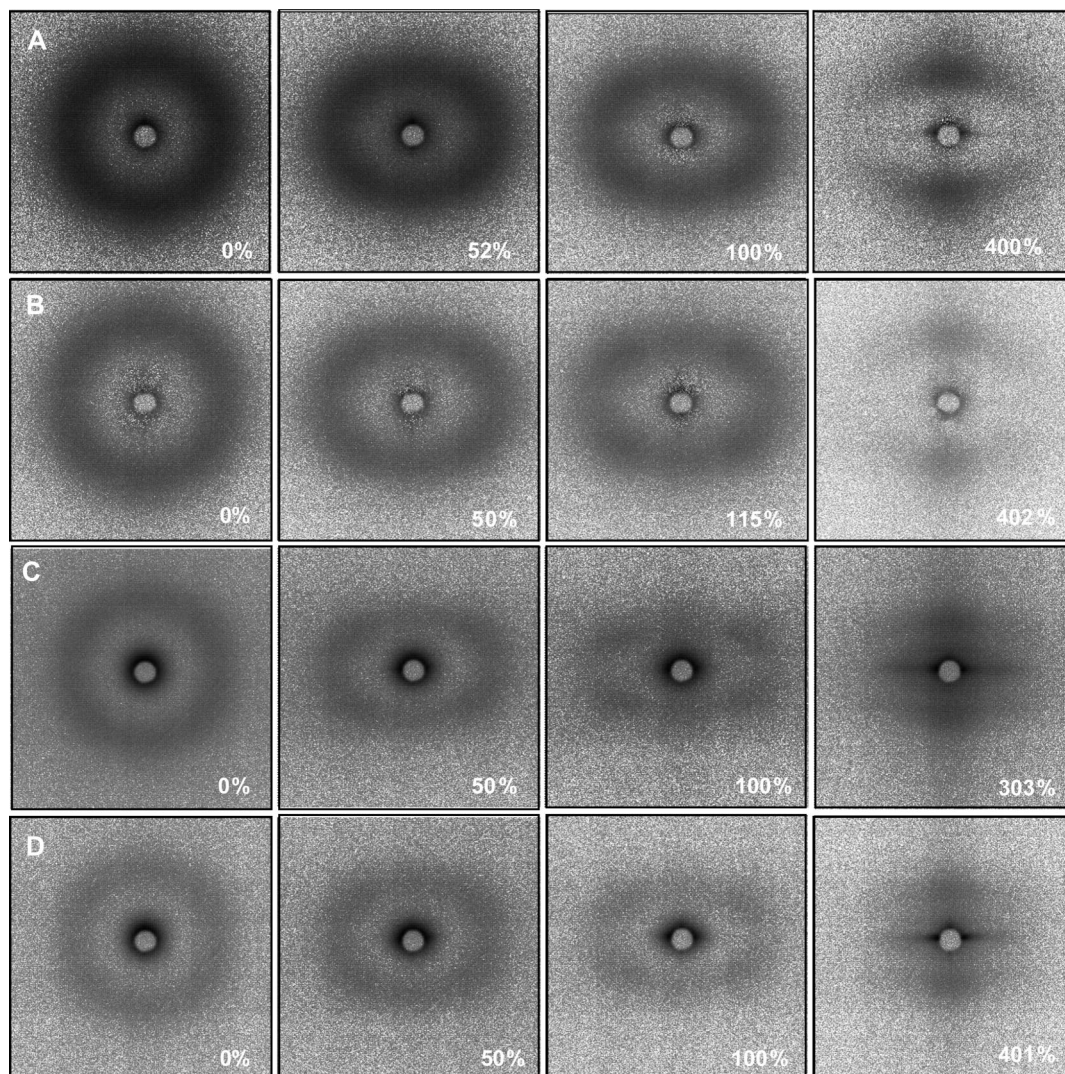


Figure 7. 2D SAXS patterns of PCLU4U at various elongations with various amounts of incorporated filler: (A) 0, B) 10, C) 23, and D) 50 mol % filler. Strain in each sample is given in percent.

soft segments, and the stacks of the first hard phase (polymer bisurea units containing a maximum amount of incorporated filler) are now pulled into a perpendicular orientation (Figure 8). The second hard phase consists of only filler and is not connected to the matrix via PCL chains. Therefore, we propose that stress cannot be transferred to the soft segments in this case, and the filler nanoribbons remain in their parallel orientation. Upon high strains, we would then have nanoribbons oriented perpendicular and parallel to the strain axis of the first and second hard phase, respectively. The excess filler no longer acts as a supramolecular filler but more as common reinforcement fillers with significantly larger-than-molecular dimensions. The results presented here and in our previous article¹⁶ show that the Young's modulus can be tuned in the first regime by mixing in supramolecular filler. During deformation, the filler and the polymer hard segments remain a single hard phase providing excellent interfacial adhesion. Therefore, the deformation mechanism of PCLU4U reinforced with supramolecular filler is similar to well-defined TPEs.

Experimental Section

Materials and General Synthetic Procedures. All reagents and solvents were purchased from commercial sources and were used without further purification. Chloroform was dried over 4 Å molsieves (Merck). All reactions were carried out under a dry argon atmosphere.

Synthesis of PCLU4U and Supramolecular Filler. The synthesis of PCLU4U and the supramolecular filler are reported elsewhere.¹⁷

Preparation of Polymer Films. All samples were prepared by dissolving the right amounts of supramolecular filler and PCLU4U together in chloroform. Films for transmission FT-IR dichroism were prepared by drop casting these solutions on glass with a mean roughness of $1 \pm 0.1 \mu\text{m}$. The thickness of the resulting films was $25 \pm 5 \mu\text{m}$. All films were annealed at 80°C in vacuo for 4 h.

Films for SAXS analysis were prepared by drop casting the appropriate solutions ($\sim 400 \text{ mg}$ in 6 mL) in Teflon dishes of $45 \times 25 \times 5 \text{ mm}^3$. The dishes were covered with a spoutless beaker to allow the solvent to evaporate slowly. After thermally annealing at 80°C in vacuo for 4 h, tensile bars were cut from the resulting films (length between 1.5 and 2.0 cm, width $\sim 5 \text{ mm}$, thickness between 0.5 and 1.0 mm).

Small-Angle X-ray Scattering. SAXS experiments were performed at the DUBBLE beam line (BM26B) at the European Synchrotron Radiation Facility (ESRF) in Grenoble, France. The 2D SAXS data were collected on a multiwire 2D detector positioned $\sim 2.5 \text{ m}$ from the sample using a wavelength of 0.954 \AA . For calibration of the SAXS detector, the positions of the diffracted peaks of a silver behenate standard sample were used. The samples were stretched using a homemade tensile test machine at an elongation rate of 10 mm/min . Samples were stretched to the mentioned elongation, and directly after that, SAXS data were collected for 5 min. As a control experiment, we also dynamically

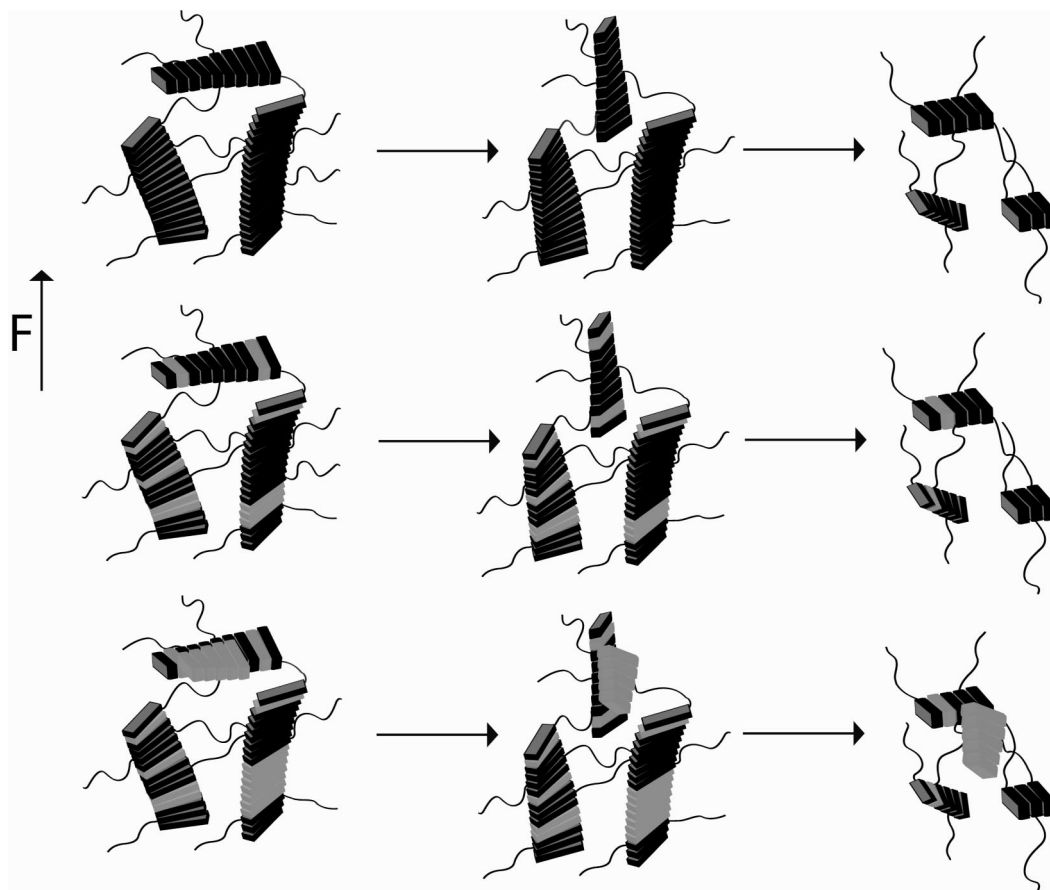


Figure 8. Schematic representation of molecular picture during deformation in the indicated direction for PCLU4U (top), PCLU4U with incorporated filler in the first regime (middle), and PCLU4U with incorporated filler in the second regime (bottom). For clarity, the nanoribbons are drawn as single supramolecular ribbons.

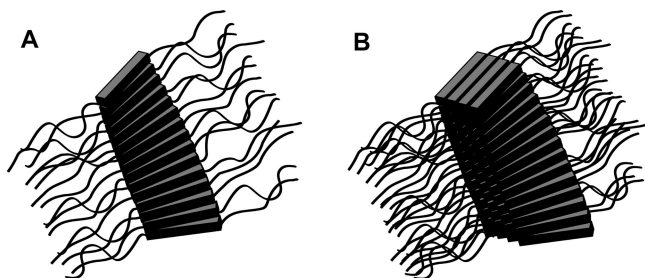


Figure 9. (A) Supramolecular ribbon of single bisurea stack and (B) proposed composition of bisurea hard segment stacks. A few bisurea ribbons form a nanoribbon.

measured SAXS data during a tensile test at a rate of 1 mm/min. All measurements were performed at 37 °C. Both methods resulted in comparable scattering patterns. In the duplo experiments, the horizontal streaks were found in only the 400% deformed samples containing 25 or 50% filler. The clamps of the apparatus moved both in the opposite direction and at the same speed so that the center position of the sample was fixed in the X-ray beam. The experimental data were at first divided by the detector response to correct for the different pixel-to-pixel sensitivity of the detector and were then corrected for the background scattering. We transformed the 2D SAXS images of the nonstretched samples into 1D profiles by performing radial integration along the azimuthal angle using the FIT2D program developed by Dr. Hammersley of the ESRF.²²

Transmission Fourier Transform Infrared Dichroism. The prepared films were uniaxially elongated in a miniaturized stretching machine, which was modified to fit in the sample compartment of the spectrometer at an elongation rate of 10 mm/min. During deformation, 10 scan interferograms were acquired in small time

intervals (2.975 s) with polarized radiation alternately changed between the parallel and perpendicular directions with respect to the deformation axis. All measurements were performed at 37 °C. Upon completion of the experiment, the interferograms were transformed to the corresponding spectra with a spectral resolution of 4 cm⁻¹. The dichroic ratio *R* (see main text) was determined as the absorbance of a specified band recorded parallel to the deformation axis, divided by the absorbance of a specified band recorded perpendicular to the deformation axis. The area of the specified band was taken as the value for *A*.

Acknowledgment. This research has been financially supported by the Council for Chemical Sciences of The Netherlands Organization for Scientific Research (NWO-CW). J. G. P. Goossens, L. E. Govaert, Brahim Mezari, Pieter C. M. M. Magusin, and R. P. Sijbesma are gratefully acknowledged for useful discussions and experimental help.

References and Notes

- (1) Bonart, R. *J. Macromol. Sci., Phys.* **1968**, B2, 115.
- (2) Bonart, R.; Morbitzer, L.; Hentze, G. *J. Macromol. Sci., Phys.* **1969**, B3, 337.
- (3) Pope, D. P.; Keller, A. *J. Polym. Sci.* **1975**, 13, 533.
- (4) Desper, C. R.; Schneider, N. S.; Jasinski, J. P.; Lin, J. S. *Macromolecules* **1985**, 18, 2755.
- (5) Seymore, R. W.; Allegranza, A. E., Jr; Cooper, S. L. *Macromolecules* **1973**, 6, 896.
- (6) Lin, S. B.; Hwang, K. S.; Tsay, S. Y.; Cooper, S. L. *Colloid Polym. Sci.* **1985**, 263, 128.
- (7) Moreland, J. C.; Wilkes, G. L.; Turner, R. B. *J. Appl. Polym. Sci.* **1991**, 43, 801.
- (8) Reynolds, N.; Spiess, H. W. *Macromol. Chem. Phys.* **1994**, 195, 2855.
- (9) Lee, H. S.; Lee, N. W.; Paik, K. H.; Ihm, D. W. *Macromolecules* **1994**, 27, 4364.

- (10) Lee, H. S.; Hsu, S. L. *J. Polym. Sci., Part B: Polym. Phys.* **1994**, *32*, 2085.
- (11) Fischer, W. B.; Pötschke, P.; Pompe, G.; Eichhorn, K.-J.; Siesler, H. W. *Macromol. Chem. Phys.* **1997**, *198*, 2057.
- (12) Numora, S.; Ashitani, R.; Matsuda, H.; Banda, L. *Polymer* **2001**, *42*, 9045.
- (13) (a) Niesten, M. C. E. J.; Harkema, S.; van der Heide, E.; Gaymans, R. J. *Polymer* **2001**, *42*, 1131. (b) Sauer, B. B.; McLean, R. S.; Gaymans, R. J.; Niesten, M. C. J. E. *J. Polym. Sci., Part B: Polym. Phys.* **2004**, *42*, 1783.
- (14) Lee, H. S.; Yoo, S. R.; Seo, S. W. *J. Polym. Sci., Part B: Polym. Phys.* **1999**, *37*, 3233.
- (15) Lee, H. S.; Park, H. D.; Cho, C. K. *J. Appl. Polym. Sci.* **2000**, *77*, 699.
- (16) Yeh, F.; Hsiao, B. S.; Sauer, B. B.; Michel, S.; Siesler, H. W. *Macromolecules* **2003**, *36*, 1940.
- (17) Wisse, E.; Govaert, L. E.; Meijer, H. E. H.; Meijer, E. W. *Macromolecules* **2006**, *39*, 7425.
- (18) Wisse, E.; Spiering, A. J. H.; van Leeuwen, E. N. M.; Renken, R. A. E.; Dankers, P. Y. W.; Brouwer, L. A.; van Luyn, M. J. A.; Harmsen, M. C.; Sommerdijk, N. A. J. M.; Meijer, E. W. *Biomacromolecules* **2006**, *7*, 3385.
- (19) (a) Magusin, P. C. M. M.; Mezari, B.; Mee, L.; Van der; Palmans, A. R. A.; Meijer, E. W. *Macromol. Symp.* **2005**, *230*, 126. (b) Wisse, E.; Spiering, A. J. H.; Dankers, P. Y. W.; Mezari, B.; Magusin, P. C. M. M.; Meijer, E. W.; manuscript in preparation.
- (20) The carbon selection made by ^1H – ^{13}C cross-polarization is never absolute. Moreover, the measurements are performed at room temperature, at which the PCL segments are still partially semicrystalline. This fact could also result in some relatively rigid PCL carbonyl carbons.
- (21) Versteegen, R. M.; Kleppinger, R.; Sijbesma, R. P.; Meijer, E. W. *Macromolecules* **2006**, *39*, 772.
- (22) The FIT2D Home Page. <http://www.esrf.eu/computing/scientific/FIT2D/index.html> .

MA801668K